TIFR/TH/98-08
March 1998

Higgs and SUSY Searches at LHC*

D.P. Roy

Tata Institute of Fundamental Research,
Homi Bhabha Road, Mumbai 400 005, India

I start with a brief introduction to Higgs mechanism and supersymmetry. Then I discuss the theoretical expectations, current limits and search strategies for Higgs boson(s) at LHC — first in the SM and then in the MSSM. Finally I discuss the signatures and search strategies for the superparticles.

* Invited talk at the 5th Workshop on High Energy Physics Phenomenology (WHEPP-5), Pune, India, 12 - 15 January 1998.

As per the Standard Model (SM) the basic constituents of matter are the quarks and leptons, which interact by the exchange of gauge bosons – photon, gluon and the massive W and Z bosons. By now we have seen all the quarks and leptons as well as the gauge bosons. But the story is not complete yet because of the mass problem.

Mass Problem (Higgs Mechanism):

The question is how to give mass to the weak gauge bosons, W and Z, without breaking gauge symmetry, which is required for a renormalisable field theory. In order to appreciate it consider the weak interaction Lagrangian of a charged scalar field ϕ; i.e.

$$\mathcal{L} = \left(\partial_\mu\phi + ig\frac{\vec{\tau}}{2}\vec{W}_\mu\phi\right)^\dagger\left(\partial_\mu\phi + ig\frac{\vec{\tau}}{2}\vec{W}_\mu\phi\right) - \left[\mu^2\phi^\dagger\phi + \lambda(\phi^\dagger\phi)^2\right] - \frac{1}{4}\vec{W}_{\mu\nu}\vec{W}_{\mu\nu}, \tag{1}$$

where

$$\vec{W}_{\mu\nu} = \partial_\mu\vec{W}_\nu - \partial_\nu\vec{W}_\mu - g\vec{W}_\mu \times \vec{W}_\nu \tag{2}$$

is the field tensor for the weak gauge bosons $\vec{W}_\mu$. The charged and the neutral W bosons form a $SU(2)$ vector, reflecting the nonabelian nature of this gauge group. This is responsbible for the last term in (2), which leads to gauge boson self-interaction. Correspondingly the gauge transformation on $\vec{W}_\mu$ has an extra term, i.e.

$$\phi \to e^{i\vec{\alpha}\cdot\vec{\tau}}\phi,\ \vec{W}_\mu \to \vec{W}_\mu - \frac{1}{g}\partial_\mu\vec{\alpha} - \vec{\alpha}\times\vec{W}_\mu. \tag{3}$$

This ensures gauge invariance of $\vec{W}_{\mu\nu}$, and hence for the last term of the Lagrangian, representing gauge kinetic energy. Evidently the middle term, representing scalar mass and self-interaction, is invariant under gauge transformation on ϕ. Finally the first term, representing scalar kinetic energy and gauge interaction, can be easily shown to be invariant under the simultaneous gauge transformations (3). However the addition of a mass term

$$-M^2\vec{W}_\mu\cdot\vec{W}_\mu, \tag{4}$$

would clearly break the gauge invariance of the Lagrangian. Note that, in contrast the scalar mass term, $\mu^2\phi^\dagger\phi$, is clearly gauge invariant. This phenomenon is exploited to give mass to the gauge bosons through back door

without breaking the gauge invariance of the Lagrangian. This is the celebrated Higgs mechanism of spontaneous symmetry breaking [1].

One starts with a $SU(2)$ doublet of complex scalar field ϕ with imaginary mass, i.e. $\mu^2 < 0$. Consequently the minimum of the scalar potential, $\mu^2\phi^\dagger\phi + \lambda(\phi^\dagger\phi)^2$, moves out from the origin to a finite value

$$v = \sqrt{-\mu^2/\lambda}, \tag{5}$$

i.e. the field develops a finite vacuum expectation value. Since the quantum perturbative expansion is stable only around a local minimum, one has to translate the field by the constant quantity,

$$\phi = v + H(x). \tag{6}$$

Thus one gets a valid perturbative field theory in terms of the redefined field H. This represents the physical Higgs boson, while the 3 other components of the complex doublet field are absorbed to give mass and hence logitudinal components to the gauge bosons.

Substituting (6) in the first term of the Lagrangian (1) leads to a mass term for W,

$$M_W = \frac{1}{2}gv. \tag{7}$$

It also leads to a HWW coupling,

$$\frac{1}{2}g^2v = gM_W, \tag{8}$$

i.e. the Higgs coupling to the gauge bosons is propertional to the gauge boson mass. Similarly its couplings to quarks and leptons can be shown to be propertional to their respective masses, i.e.

$$h_{\ell,q} = m_{\ell,q}/v = \frac{1}{2}gm_{\ell,q}/M_W. \tag{9}$$

Indeed, this is the source of the fermion masses in the SM. Finally substituting (6) in the middle term of the Lagrangian leads to a real mass for the physical Higgs boson,

$$M_H = v\sqrt{2\lambda} = M_W(2\sqrt{2\lambda}/g). \tag{10}$$

Substituting $M_W = 80$ GeV and $g = 0.65$ along with a perturbative limit on the scalar self-coupling $\lambda \lesssim 1$, implies that the Higgs boson mass is bounded by $M_H < 1000$ GeV. But the story does not end here. Giving mass to the gauge bosons via the higgs mechanism leads to the so called hierarchy problem.

Hierarchy Problem (Supersymmetry):

The problem is how to peg down the Higgs scalar in the desired mass range of a few hundered GeV. This is because the scalar masses are known to have quadratically divergent quantum corrections from radiative loops involving e.g. quarks or leptons. These would push the output scalar mass to the cut-off scale of the SM, i.e. the GUT scale (10^{16} GeV) or the Planck scale (10^{19} GeV). The desired mass range of $\sim 10^2$ GeV is clearly tiny compared to these scales. This is the so called hierarchy problem. The underlying reason for the quadratic divergence is that the scalar masses are not protected by any symmetry unlike the fermion and the gauge boson masses, which are protected by chiral symmetry and gauge symmetry. Of course it was this very property of the scalar mass that was exploited to give masses to the fermions and gauge bosons in the first place. Therefore it can not be simply wished away.

The most attractive solution to this problem is provided by supersymmetry (SUSY), a symmetry between fermions and bosons [2]. It predicts the quarks and leptons to have scalar superpartners called squarks and sleptons $(\tilde{q}, \tilde{\ell})$, and the gauge bosons to have fermionic superpartners called gauginos $(\tilde{g}, \tilde{\gamma}, \tilde{W}, \tilde{Z})$. In the minimal supersymmetric extension of the standard model (MSSM) one needs two Higgs doublets $H_{1,2}$, with opposite hypercharge $Y = \pm 1$, to give masses to the up and down type quarks. The corresponding fermionic superpartners are called Higgsinos $(\tilde{H}_{1,2})$. The opposite hypercharge of these two sets of fermions ensures anomaly cancellation.

SUSY ensures that the quadratically divergent quantum corrections from quark and lepton loops are cancelled by the contributions from the corresponding squark and slepton loops. Thus the Higgs masses can be kept in the desired range of $\sim 10^2$ GeV. However this implies two important constraints on SUSY breaking.

i) SUSY can be broken in masses but not in couplings (soft breaking), so that the co-efficients of the cancelling contributions remain equal and

opposite.

ii) The size of SUSY breaking in masses is $\sim 10^2$ GeV, so that the size of the remainder remains within this range. Thus the superpartners of the SM particles are also expected to lie in the mass range of $\sim 10^2$ GeV, going upto 1000 GeV.

SM Higgs Boson: Theoretical Constraints & Search Strategy

The Higgs self coupling λ is ultra-violet divergent. It evolves according to the renormalisation group equation (RGE)

$$\frac{d\lambda}{d\ell n(\mu/M_W)} = \frac{3\lambda^2}{2\pi^2}. \tag{11}$$

It can be easily solved to give

$$\lambda(\mu) = \frac{1}{1/\lambda(M_W) - (3/2\pi^2)\ell n(\mu/M_W)}, \tag{12}$$

which has a Landau pole at

$$\begin{aligned} \mu_\infty &= M_W e^{2\pi^2/3\lambda(M_W)}, \\ \lambda(M_W) &= \frac{g^2}{8}\frac{M_H^2}{M_W^2}. \end{aligned} \tag{13}$$

Thus the larger the starting value $\lambda(M_W)$, the sooner will the coupling diverge. This is illustrated in Fig. 1. Evidently the theory is valid only upto a cut-off scale $\wedge = \mu_\infty$. Requiring the theory to be valid at all energies, $\wedge \to \infty$, would imply $\lambda(M_W) \to 0$; i.e. the only good $\lambda\phi^4$ theory is a trivial theory. Surely we do not want that. But if we want the theory to be valid upto the Planck scale or GUT scale, we must have a relatively small $\lambda(M_W)$, which corresponds to a small $M_H \lesssim 200$ GeV. If on the other hand we assume it to be valid only upto the TeV scale, then we can have a larger $\lambda(M_W)$, corresponding to a relatively large $M_H \lesssim 600$ GeV. This is the so-called triviality bound [3]. If M_h is significantly larger than 600 GeV, then the range of validity of the theory is limited to $\wedge < 2M_H$. This would correspond to a composite Higgs scenario, e.g. technicolour models.

Fig. 2 shows the triviality bound on the Higgs mass against the cut-off scale $\wedge$ of the theory [4]. It also shows a lower bound on the Higgs mass, which comes from a negative contribution to the RGE (11) from the top Yukawa coupling, i.e.

$$\frac{d\lambda}{d\ell n(\mu/M_W)} = \frac{3}{2\pi^2}(\lambda^2 + \lambda h_t^2 - h_t^4). \tag{14}$$

The Yukawa coupling being ultra-violet divergent turns λ negative at a high energy scale; and the smaller the starting value of λ (or equivalently M_H) the sooner will it become negative. A negative λ coupling has the undesirable feature of an unstable vacuum (eq. 5). Thus one can define a cut-off scale $\wedge$ for the theory, where this change of sign occurs. The lower curve of Fig. 2 shows the lower bound on M_H as a function of the cut-off scale $\wedge$ including the theoretical uncertainty [5]. We see from this figure that the longer the range of validity of the theory, the stronger will be the upper and lower bounds on M_H. Thus assuming no new physics upto the GUT or Planck scale (the desert scenario) would constrain the SM Higgs mass to lie in the range

$$M_H = 130 - 190 \text{ GeV}. \tag{15}$$

However the lower bound becomes invalid once we have more than one Higgs doublet, since the unique relation between the top mass and Yukawa coupling (9) will no longer hold. In particular, one expects an upper bound of $\sim$ 130 GeV for the lightest Higgs boson mass in MSSM in stead of a lower bound, as we shall see below. Since one needs SUSY or some other form of new physics to stabilize the Higgs mass, the above vacuum stability bound may have limited significance. Nonetheless it is interesting to note that the predicted range of the SM Higgs boson mass (15) agrees favourably with the indirect estimate of this quantity from the precision measurement of electro-weak parameters at LEP/SLD [6], i.e.

$$M_H = 115^{+116}_{-66} \text{ GeV } (< 420 \text{ GeV at } 95\% \text{ CL}). \tag{16}$$

It should be added however that there is a lingering discrepancy between the LEP and the SLD values of $\sin^2\theta_W$, which could affect the central value and the 95% CL limit of M_H appreciably. Thus all one can say at the moment is that these indirect estimates are consistent with a relatively light Higgs boson.

The search strategy for Higgs boson is based on its preferential coupling to the heavy quarks and gauge bosons as seen from (8,9). The LEP-I search was based on the so called Bjorken process

$$e^+e^- \to Z \to HZ^\star \to \bar{b}b(\ell^+\ell^-, \nu\nu, \bar{q}q), \tag{17}$$

while the LEP-II search is based on the associated process with Z and $Z^\star$ intercharged. The current LEP-II limit from the preliminary ALEPH data at 183 GeV is [7]

$$M_W > 88.6 \text{ GeV}. \tag{18}$$

The forthcoming runs at $192 - 200$ GeV are expected to extend the search upto

$$M_H = 95 - 100 \text{ GeV}. \tag{19}$$

Thus the Higgs mass range of interest to LHC is $M_H \gtrsim 90$ GeV. Fig. 3 shows the total decay width of the Higgs boson over this range along with the branching ratios for the important decay channels [8]. It is clear from this figure that the mass range can be divided into two parts – a) $M_H < 2M_W(90 - 160 \text{ GeV})$ and b) $M_H > 2M_W(160 - 1000 \text{ GeV})$.

The first part is the so called intermediate mass region, where the Higgs width is expected to be only a few MeV. The dominant decay mode is $H \to \bar{b}b$. This has unfortunately a huge QCD background, which is ~ 1000 times larger than the signal. By far the cleanest channel is $\gamma\gamma$, where the continuum background is a 2nd order EW process. However, it suffers from a small branching ratio

$$B(H \to \gamma\gamma) \sim 1/1000, \tag{20}$$

since it is a higher order process, induced by the top quark loop. So one needs a very high jet/γ rejection factor $\gtrsim 10^8$. Besides the continuum background being propertional to $\Delta M_{\gamma\gamma}$, one needs a high resolution,

$$\Delta M_{\gamma\gamma} \lesssim 1 \text{ GeV i.e. } \lesssim 1\% \text{ of } M_H. \tag{21}$$

This requires fine EM calorimetry, capable of measuring the γ energy and direction to 1% accuracy. In this respect CMS is expected to do better than ATLAS. The projected Higgs mass reach of the two detectors via this channel are $M_H = 90 - 140$ GeV (CMS) and $110 - 140$ GeV (ATLAS) at the high luminosity run of LHC ($100 fb^{-1}$).

One can get a feel for the size of the signal from the Higgs production cross-sections shown in Fig. 4. The relevant production processes are

$$gg \xrightarrow{\bar{t}^\star t^\star} H, \tag{22}$$

$$qq \xrightarrow{W^\star W^\star} Hqq, \tag{23}$$

$$q\bar{q}' \xrightarrow{W^\star} HW, \tag{24}$$

$$gg, q\bar{q} \to Ht\bar{t}(Hb\bar{b}). \tag{25}$$

The largest cross-section, coming from gluon-gluon fusion via the top quark loop (22), is of the order of $10pb$. Thus the expected size of the $H \to \gamma\gamma$ signal is $\sim 10fb$, corresponding to $\sim 10^3$ events. The estimated continuum background is $\sim 10^4$ events, which can of course be subtracted out. Thus the significance of the signal is given by its relative size with respect to the statistical uncertainty in the background, i.e.

$$S/\sqrt{B} \simeq 10. \tag{26}$$

By far the cleanest signal is provided by the associated Bjorken process (24), with a cross-section of $\sim 1fb$ in the $H \to \gamma\gamma$ channel. Combining this with the BR of $2/9$ for $W \to \ell\nu$ implies a signal of $20 - 30$ events in the $\ell + \gamma\gamma$ channel. While the signal size is admittedly small, the estimated background is only ~ 10 events. Thus the $S/\sqrt{B}$ ratio is again ~ 10. Detailed signal and background simulations for these channels can be found in [9]. The result is summarised in Fig. 5. It shows that one expects a 5σ signal upto a Higgs mass of 150 GeV for an integrated Luminosity of $30fb^{-1}$. This corresponds to the low luminosity run of LHC over the first 3 years. It may be noted that the dominant decay channel, $H \to b\bar{b}$, can be important for Higgs search below 100 GeV. It comes from the associated Bjorken process (24), where the leptonic decay of the accompanying $W(Z)$ helps to reduce the background. However this region should be already covered by LEP-II.

The most promising Higgs decay channel is

$$H \to ZZ \to \ell^+\ell^-\ell^+\ell^-, \tag{27}$$

since reconstruction of the $\ell^+\ell^-$ invariant masses makes it practically background free. Thus it provides the most important Higgs signal right from

the subthresold region of $M_H = 140$ GeV upto 600 GeV (see Fig. 3). Note however a sharp dip in the ZZ branching ratio at $M_H = 160 - 170$ GeV due to the opening of the WW channel. The most important Higgs signal in this dip region is expected to come from [10]

$$H \to WW \to \ell^+ \nu \ell^- \bar{\nu}. \tag{28}$$

However in general this channel suffers from a much larger background for two reasons – i) it is not possible to reconstruct the W masses because of the two neutrinos and ii) there is a large WW background from $t\bar{t}$ decay.

For large Higgs mass, $M_H = 600 - 1000$ GeV, the 4-lepton signal (27) becomes too small in size. In this case the decay channels

$$H \to WW \to \ell \nu q \bar{q}', \quad H \to ZZ \to \ell^+ \ell^- q \bar{q}, \tag{29}$$

are expected to provide more favourable signals. The biggest background comes from single $W(Z)$ production along with QCD jets. However, one can exploit the fact that a large part of the signal cross-section in this case comes from WW fusion (23), which is accompanied by two forward (large-rapidity) jets. One can use the double forward jet tagging to effectively control the background. Indeed simulation studies by the CMS and ATLAS collaborations show that using this strategy one can extend the Higgs search right upto 1000 GeV [9].

MSSM Higgs Bosons: Theoretical Constraints & Search Strategy

As mentioned earlier, the MSSM contains two Higgs doublets, which correspond to 8 independent states. After 3 of them are absorbed by the W and Z bosons, one is left with 5 physical states: two neutral scalars h^0 and H^0, a pseudoscalar A^0, and a pair of charged Higgs scalars $H^\pm$. At the tree-level their masses and couplings are determined by only two parameters – the ratio of the two vacuum expectation values, $\tan\beta$, and one of the scalar masses, usually taken to be M_A. However, the neutral scalars get a large radiative correction from the top quark loop along with the top squark (stop) loop. To a good approximation this is given by [11]

$$\epsilon = \frac{3g^2 m_t^4}{8\pi^2 M_W^2} \ell n \left(1 + \frac{M_{\tilde{t}}^2}{m_t^2}\right), \tag{30}$$

plus an additional contribution from the $\tilde{t}_{L,R}$ mixing,

$$\epsilon_{\rm mix} = \frac{3g^2 m_t^4}{8\pi^2 M_W^2}\frac{A_t^2}{M_{\tilde{t}}^2}\left(1 - \frac{A_t^2}{12 M_{\tilde{t}}^2}\right) \leq \frac{9g^2 m_t^4}{8\pi^2 M_W^2}. \tag{31}$$

Thus while the size of $\epsilon_{\rm mix}$ depends on the trilinear SUSY breaking parameter A_t, it has a maximum value independent of A_t. As expected the radiative corrections vanish in the exact SUSY limit. One can estimate the rough magnitude of these corrections assuming a SUSY breaking scale of $M_{\tilde{t}} = 1$ TeV. The leading log QCD corrections can be taken into account by using the running mass of top at the appropriate energy scale [11]; i.e. $m_t(\sqrt{m_t M_{\tilde{t}}}) \simeq$ 157 GeV in (30) and $m_t(M_{\tilde{t}}) \simeq 150$ GeV in (31) instead of the top pole mass of 175 GeV. One can easily check that the resulting size of the radiative corrections are

$$\epsilon \sim M_W^2 \quad \text{and} \quad 0 < \epsilon_{\rm mix} \lesssim M_W^2. \tag{32}$$

The neutral scalar masses are obtained by diagonalising the mass-squared matrix

$$\begin{pmatrix} M_A^2 \sin^2\beta + M_Z^2 \cos^2\beta & -(M_A^2 + M_Z^2)\sin\beta\cos\beta \\ -(M_A^2 + M_Z^2)\sin\beta\cos\beta & M_A^2\cos^2\beta + M_Z^2\sin^2\beta + \epsilon' \end{pmatrix} \tag{33}$$

with $\epsilon' = (\epsilon + \epsilon_{\rm mix})/\sin^2\beta$. Thus

$$\begin{aligned} M_h^2 &= \frac{1}{2}\Big[M_A^2 + M_Z^2 + \epsilon' - \Big\{(M_A^2 + M_Z^2 + \epsilon')^2 - 4M_A^2 M_Z^2\cos^2\beta \\ &\qquad - 4\epsilon'(M_A^2\sin^2\beta + M_Z^2\cos^2\beta)\Big\}^{1/2}\Big] \\ M_H^2 &= M_A^2 + M_Z^2 + \epsilon' - M_h^2 \\ M_{H^\pm}^2 &= M_A^2 + M_W^2 \end{aligned} \tag{34}$$

where h denotes the lighter neutral scalar [12]. One can easily check that its mass has an upper bound for $M_A \gg M_Z$, i.e.

$$M_h^2 \longrightarrow M_Z^2\cos^2 2\beta + \epsilon + \epsilon_{\rm mix}, \tag{35}$$

while M_H^2, $M_{H^\pm}^2 \to M_A^2$. Thus the MSSM contains at least one light Higgs boson h, whose tree-level mass limit $M_h < M_Z$, goes upto $130 - 140$ GeV

after including the radiative corrections. Fig. 6 shows the masses of the MSSM Higgs bosons against M_A for two representative values of $\tan\beta = 1.5$ and 30. The predictions without stop mixing and with maximal mixing are shown in separate plots. Note that the h mass limit is particularly strong in the low $\tan\beta$ (~ 1) region, i.e. $M_h < 80 - 100$ GeV depending on the size of stop mixng parameter A_t. Consequently the low $\tan\beta$ region is particularly succeptible to the ongoing Higgs search at LEP-II as we shall see below.

Let us consider now the couplings of the MSSM Higgs bosons. A convenient parameter for this purpose is the mixing angle α between the neutral scalars, i.e.

$$\tan 2\alpha = \tan 2\beta \frac{M_A^2 + M_Z^2}{M_A^2 - M_Z^2 + \epsilon'/\cos 2\beta}, -\pi/2 < \alpha < 0. \tag{36}$$

Note that

$$\alpha \stackrel{M_A \gg M_Z}{\longrightarrow} \beta - \pi/2. \tag{37}$$

Table-I. Important couplings of the MSSM Higgs bosons h, H and A relative to those of the SM Higgs boson

Channel	$H_{\rm SM}$	h	H	A
$\bar{b}b(\tau^+\tau^-)$	$\frac{gm_b}{2M_W}(m_\tau)$	$\sin\alpha/\cos\beta$ $\to 1$	$\cos\alpha/\cos\beta$ $\tan\beta$	$\tan\beta$ "
$\bar{t}t$	$g\frac{m_t}{2M_W}$	$\cos\alpha/\sin\beta$ $\to 1$	$\sin\alpha/\sin\beta$ $\cot\beta$	$\cot\beta$ "
$WW(ZZ)$	$gM_W(M_Z)$	$\sin(\beta-\alpha)$ $\to 1$	$\cos(\beta-\alpha)$ 0	0 "

Table-I shows the important couplings of the neutral Higgs bosons relative to those of the SM Higgs boson. The limiting values of these couplings at large M_A are indicated by arrows. The corresponding couplings of the charged Higgs boson, which has no SM analogue, are

$$\begin{aligned} H^+\bar{t}b &: \frac{g}{\sqrt{2}M_W}(m_t \cot\beta + m_b \tan\beta),\ H^+\tau\nu : \frac{g}{\sqrt{2}M_W} m_\tau \tan\beta, \\ H^+W^-Z &: 0. \end{aligned} \tag{38}$$

Note that the top Yukawa coupling is ultraviolet divergent. Assuming it to lie within the perturbation theory limit all the way upto the GUT scale implies

$$1 < \tan\beta < m_t/m_b, \tag{39}$$

which is therefore the favoured range of $\tan\beta$. However, it assumes no new physics beyond the MSSM upto the GUT scale, which is a stronger assumption than MSSM itself. Nontheless we shall concentrate in this range.

Coming back to the neutral Higgs couplings of Table-I, we see that in the large M_A limit the light Higgs boson (h) couplings approach the SM values. The other Higgs bosons are not only heavy, but their most important couplings are also suppressed. This is the so called decoupling limit, where the MSSM Higgs sector is phenomenologically indistinguishable from the SM. It follows therefore that the Higgs search stategy for $M_A \gg M_Z$ should be the same as the SM case, i.e. via

$$h \to \gamma\gamma. \tag{40}$$

At lower M_A, several of the MSSM Higgs boson become light. Unfortunately their couplings to the most important channels, $\bar{t}t$ and WW/ZZ, are suppressed relative to the SM Higgs boson [12]. Thus their most important production cross-sections as well as their decay BRs into the $\gamma\gamma$ channel are suppressed relative to the SM case. Consequently the Higgs detection in this region is very hard and it calls for multiprong stategy from the three sides in the $M_A - \tan\beta$ plane (Fig. 7): (a) Low M_A, (b) High $\tan\beta$ and (c) Low $\tan\beta$.

(a) Low $M_A(\lesssim M_Z)$ – In this case $M_{H^\pm} < M_t$; and the best strategy is to search for $H^\pm$ in top quark decay, i.e.

$$t \to bH^+,\ H^+ \to \tau\nu, \tag{41}$$

via preferential top decay into the τ channel as well as the opposite polarization of τ wrt the SM decay ($W \to \tau\nu$) [14].

(b) High $\tan\beta(\sim m_t/m_b)$ – It is clear from Table-I that in this case the best production and decay channels are

$$gg \to b\bar{b}(h, H, A) \to b\bar{b}\tau^+\tau^-. \tag{42}$$

(c) Low $\tan\beta(\sim 1)$ – As mentioned earlier the LEP-II search via the associated Bjorken process becomes very effective in this case. Indeed one can see from (36) that in this case (37) holds even for relatively low M_A, so that the hZZ coupling is very close to the SM case. Thus the present LEP-II limit (18) as well as the discovery limit (19) are equally valid for M_h in the low $\tan\beta$ region. As one can see from Fig. 6, the former rules out the $\tan\beta \lesssim 1.5$ region for the no stop-mixing case while the latter will rule it out even for the maximal stop mixing case. It may be added here that a modest part of the large $\tan\beta$ region seems to be ruled out as well by the Tevatron data via (41) [15] and (42) [16].

Fig. 7 summarises the MSSM Higgs discovery limits of the CMS detector at LHC via the three processes (40-42) along with the LEP-II limit. Note that there is a significant hole in the $M_A - \tan\beta$ plane that is left out even after combining all the 4 limits. Moreover the LEP-II limit will go down to a lower range of $\tan\beta$ when stop mixing effect is taken into account (Fig. 6). This will enlarge the size of the hole further. Finally, Fig. 8 shows that it would be possible to close the hole if one combines the CMS and the ATLAS data collected over an integrated luminosity of $300 fb^{-1}$ [17]. This corresponds to 3 years of high luminosity run of LHC; and illustrates the challenge involved in the search for the MSSM Higgs bosons. Note that even in this case there is a large region where one would see only one Higgs boson (h) with SM like couplings and hence not be able to distinguish the SUSY from the SM Higgs sector. Fortunately it will be possible and in fact much easier to probe SUSY directly via superparticle search as we see below.

Superparticles: Signature Search Strategy

I shall concentrate on the standard SUSY model, where the superparticle signature is based on R-parity conservation. Let me start therefore with a

brief discussion of R-parity. The presence of scalar quarks in SUSY can lead to baryon and lepton number violating interactions of the type $ud \to \tilde{\bar{s}}$ and $\tilde{\bar{s}} \to e^+\bar{u}$, i.e.

$$ud \xrightarrow{\tilde{\bar{s}}} e^+\bar{u}. \tag{43}$$

Moreover adding a spectator u quark to both sides one sees that this can lead to a catastrophic proton decay, i.e.

$$p(uud) \xrightarrow{\tilde{\bar{s}}} e^+\pi^0(\bar{u}u). \tag{44}$$

Since the superparticle masses are assumed to be of the order M_W for solving the hierarchy problem, this would imply a proton life time similar to the typical weak decay time of $\sim 10^{-8}$sec! The best way to avoid this catastrophic proton decay is via R-parity conservation, where

$$R = (-1)^{3B+L+2S} \tag{45}$$

is defined to be $+1$ for the SM particles and -1 for their superpartners, since they differ by $1/2$ unit of spin S. It automatically ensures L and B conservation by preventing single emission (absorption) of superparticle.

Thus R-conservation implies that (i) superparticles are produced in pair and (ii) the lightest superparticle (LSP) is stable. Astrophysical evidences against such a stable particle carrying colour or electric charge imply that the LSP is either sneutrino $\tilde{\nu}$ or photino $\tilde{\gamma}$ (or in general the lightest neutralino). The latter alternative is favoured by the present SUSY models. In either case the LSP is expected to have only weak interaction with ordinary matter like the neutrino, since e.g.

$$\tilde{\gamma}q \xrightarrow{\tilde{q}} q\tilde{\gamma} \quad \text{and} \quad \nu q \xrightarrow{W} eq' \tag{46}$$

have both electroweak couplings and $M_{\tilde{q}} \sim M_W$. This makes the LSP an ideal candidate for the cold dark matter. It also implies that the LSP would leave the normal detectors without a trace like the neutrino. The resulting imbalance in the visible momentum constitutes the canonical missing transverse-momentum ($\not{p}_T$) signature for superparticle production at hadron colliders. It is also called the missing transverse-energy ($\not{E}_T$) as it is often measured as a vector sum of the calorimetric energy deposits in the transverse plane.

The main processes of superparticle production at LHC are the QCD processes of quark-antiquark and gluon-gluon fusion [18]

$$q\bar{q}, gg \longrightarrow \tilde{q}\bar{\tilde{q}}(\tilde{g}\tilde{g}). \tag{47}$$

The NLO corrections can increase these cross-sections by $15-20\%$ [19]. The simplest decay processes for the produced squarks and gluinos are

$$\tilde{q} \to q\tilde{\gamma},\ \tilde{g} \to q\bar{q}\tilde{\gamma}. \tag{48}$$

Convoluting these with the pair production cross-sections (47) gives the simplest jets + $\not{p}_T$ signature for squark/gluino production, which were adequate for the early searches for relatively light squarks and gluinos. However, over the mass range of current interest (≥ 100 GeV) the cascade decays of squark and gluino into the LSP via the heavier chargino/neutralino states are expected to dominate over the direct decays (48). This is both good news and bad news. On the one hand the cascade decay degrades the missing-p_T of the canonical jets $+\not{p}_T$ signature. But on the other hand it gives a new multilepton signature via the leptonic decays of these chargino/neutralino states. It may be noted here that one gets a mass limit of

$$M_{\tilde{q},\tilde{g}} > 180 \text{ GeV} \tag{49}$$

from the Tevatron data using either of the two signatures [20].

The cascade decay is described in terms of the $SU(2) \times U(1)$ gauginos $\tilde{W}^{\pm,0}, \tilde{B}^0$ along with the Higgsinos $\tilde{H}^{\pm}$, $\tilde{H}_1^0$ and $\tilde{H}_2^0$. The $\tilde{B}$ and $\tilde{W}$ masses are denoted by M_1 and M_2 respectively while the Higgsino masses are functions of the supersymmetric Higgsino mass parameter μ and $\tan\beta$. The charged and the neutral gauginos will mix with the corresponding Higgsinos to give the physical chargino $\chi_{1,2}^{\pm}$ and neutralino $\chi_{1,2,3,4}^0$ states. Their masses and compositions can be found by diagonalising the corresponding mass matrices, i.e.

$$M_C = \begin{pmatrix} M_2 & \sqrt{2}M_W \sin\beta \\ \sqrt{2}M_W \cos\beta & \mu \end{pmatrix},$$

$$M_N = \begin{pmatrix} M_1 & 0 & -M_Z \sin\theta_W \cos\beta & M_Z \sin\theta_W \sin\beta \\ 0 & M_2 & M_Z \cos\theta_W \cos\beta & -M_Z \cos\theta_W \sin\beta \\ -M_Z \sin\theta_W \cos\beta & M_Z \cos\theta_W \cos\beta & 0 & -\mu \\ M_Z \sin\theta_W \sin\beta & -M_Z \cos\theta_W \sin\beta & -\mu & 0 \end{pmatrix}. \tag{50}$$

Let me try to present a simplified picture. Assuming unification of the $SU(3) \times SU(2) \times U(1)$ gaugino masses at the GUT scale the RGE relates the corresponding masses at the low energy scale ($\sim 10^2$ GeV) to the respective gauge couplings. Thus

$$\begin{aligned} M_2 &= (g^2/g_S^2) M_{\tilde{g}} \simeq 0.3 M_{\tilde{g}} \\ M_1 &= (5 \tan^2\theta_W/3) M_2 \simeq 0.5 M_2. \end{aligned} \tag{51}$$

Moreover the SUGRA assumptions of a common scalar mass at the GUT scale along with the radiative breaking of the EW symmetry (5), imply

$$\mu \gg M_2. \tag{52}$$

It is clear from (50,51,52) that the lighter chargino and neutralino states are expected to be dominated by gaugino components. In particular

$$\begin{aligned} \chi^{\pm}_{1,2} &\simeq \tilde{W}^{\pm}, \tilde{H}^{\pm} \\ \chi^0_{1,2,\cdots} &\simeq \tilde{B}, \tilde{W}^0, \cdots \end{aligned} \tag{53}$$

With the above systematics one can understand the essential features of cascade decay. For illustration I shall briefly discuss cascade decay of gluino for two representative gluino mass regions of interest to LHC.

i) $M_{\tilde{g}} \simeq 300$ GeV: In this case the gluino decays into the light quarks

$$g \to \bar{q}q \left[\tilde{B}(.2), \tilde{W}^0(.3). \tilde{W}^{\pm}(.5)\right], \; q \neq t, \tag{54}$$

which have negligible Yukawa couplings. Thus the decay branching ratios are propertional to the squares of the respective gauge couplings

as indicated in parantheses. Because of the smaller $U(1)$ gauge coupling relative to the $SU(2)$, the direct decay into the LSP ($\tilde{B}$) is small compared to cascade decay via the heavier ($\tilde{W}$ dominated) chargino and neutralino states. The latter decay into the LSP via real or virtual W/Z emission,

$$\tilde{W}_0 \to Z\tilde{B} \to \ell^+\ell^-\tilde{B}(.06),\ \tilde{W}^\pm \to W\tilde{B} \to \ell^\pm\nu\tilde{B}(.2), \qquad (55)$$

whose leptonic branching ratios are indicated in parantheses. From (54) and (55) one can easily calculate the branching ratios of dilepton and trilepton states resulting from the decay of a gluino pair. In particular the dilepton final state has a branching ratio of 1%. Then the Majorana nature of $\tilde{g}$ implies a distinctive like sign dilepton (LSD) signal with a BR of $\sim 1/2\%$.

ii) $\tilde{M_{\tilde{g}}} \gtrsim 500$ GeV: In this case the large top Yukawa coupling implies a significant decay rate via

$$\tilde{g} \to t\bar{b}\tilde{H}^-, \qquad (56)$$

where both t and $\tilde{H}^-$ can contribute to the leptonic final state via

$$t \to bW^+ \to b\ell^+\nu(.2),\ \tilde{H}^- \to W^-\tilde{B} \to \ell^-\nu\tilde{B}(.2). \qquad (57)$$

Consequently the BR of the LSD signal from the decay of the gluino pair is expected to go up to $3-4\%$.

Fig. 9 shows the expected LSD signal from gluino pair production at LHC for $M_{\tilde{g}} = 300$ and 800 GeV along with the background [21]. The latter comes from $\bar{t}t$ via cascade decay (long dashed) or charge misidentification (dots). Note that the signal is accompanied by a much larger $\not{p}_T$ compared to the background because of the LSPs. This can be used to effectively suppress the background while retaining about 1/2 of the signal. Consequently one can search for a gluino upto at least 800 GeV at the low luminosity ($10fb^{-1}$) run of LHC, going upto 1200 GeV at the high luminosity ($100fb^{-1}$).

Fig. 10 shows the size of the canonical $\not{p}_T$+ jets signal against gluino mass for two cases – $M_{\tilde{g}} \ll M_{\tilde{q}}$ (triangles) and $M_{\tilde{g}} \simeq M_{\tilde{q}}$ (squares) [22]. The background line shown also corresponds to $5\sqrt{B}$ for the LHC luminosity of $10fb^{-1}$. Thus one expects a 5σ discovery limit of at least upto $M_{\tilde{g}} =$

1300 GeV from this signal[1]. Finally, Fig. 11 shows the CMS simulation for the 5σ discovery limits from the various leptonic channels in the plane of $m_0 - m_{1/2}$, the common scalar and gaugino masses at the GUT scale. The corresponding squark and gluino mass contours are also shown. As we see from this figure, it will be possible to extend the squark and gluino searches at LHC well into the TeV region. One should either see these superparticles or rule out SUSY at least as a solution to the hierarchy problem of the SM.

I am thankful to Dr. D. Denegri of the CMS collaboration for providing figures 7 and 11. I also thank R.S. Pawar and S.K. Vempathi for help in plotting figures 1 and 6 and S. Datta for embedding the figure files.

[1]This signal may be hard to observe at the high luminosity run due to event pileup.

References:

1. For a review see e.g. J.F. Gunion, H.E. Haber, G. Kane and S. Dawson, The Higgs Hunters' Guide (Addison-Wesley, Reading, MA, 1990).

2. For a review see e.g. H.E. Haber and G. Kane, Phys. Rep. 117, 75 (1985).

3. L. Maiani, G. Parisi and R. Petronzio, Nucl. Phys. B136, 115 (1978); N. Cabbibo, L. Maiani, G. Parisi and R. Petronzio, Nucl. Phys. B158, 295 (1979); M. Lindner, Z. Phys. C31, 295 (1986).

4. K. Riesselmann, hep-ph/9711456 (to appear in Proc. 35th Intl. School of Subnuclear Physics, Erice, 1997). For the theoretical uncertainty in the upperbound see T. Hambye and K. Riesselmann, Phys. Rev. D55, 7255 (1997).

5. G. Altarelli and G. Isidori, Phys. Lett. B337, 141 (1994); J.A. Casas, J.R. Espinosa and M. Quiros, Phys. Lett. B342, 171 (1995) and B382, 374 (1996).

6. LEP Electroweak Working Group and SLD Heavy Flavour Group, CERN-PPE/97-154 (2 Dec. 1997).

7. P. Janot, Invited talk at the Indo-French Workshop on Supersymmetry and Unification, TIFR, Mumbai (17-21 Dec. 1997).

8. M. Spira, hep-ph/9705337.

9. CMS Technical Proposal, CERN/LHCC/94-38 (1994); ATLAS Technical Proposal, CERN/LHCC/94-43 (1994).

10. M. Dittmar and H. Dreiner, Phys. Rev. D55, 167 (1997).

11. For a recent review of radiative correction along with reference to the earlier works see H.E. Haber, R. Hempfling and A.H. Hoang, Z. Phys. C75, 539 (1997).

12. See e.g. A. Djouadi, J. Kalinowski and P.M. Zerwas, Z. Phys. C70, 435 (1996).

13. Simulation study by the CMS collaboration.

14. D.P. Roy, Phys. Lett. 277B, 183 (1992) and Phys. Lett. 283B, 403 (1992); S. Raychaudhuri and D.P. Roy, Phys. Rev. D53, 4902 (1996).

15. M. Guchait and D.P. Roy, Phys. Rev. D55, 7263 (1997); CDF Collaboration: F. Abe et al., Phys. Rev. Lett. 79, 357 (1997).

16. M. Drees, M. Guchait and P. Roy, hep-ph/9801229.

17. E. Richt-Was et al., CERN-TH-96-111 (1996).

18. G.L. Kane and J.P. Leville, Phys. Lett. B112, 227 (1982); P.R. Harrison and C.H. Llewellyn-Smith, Nucl. Phys. B213, 223 (1983) [Err. Nucl. Phys. B223, 542 (1983)]; E. Reya and D.P. Roy, Phys. Rev. D32, 645 (1985).

19. W. Beenakker, R. Hopker, M. Spira and P. Zerwas, Nucl. Phys. B492, 51 (1997); M. Kramer, T. Plehn, M. Spira and P. Zerwas, Phys. Rev. Lett. 79, 341 (1997).

20. CDF and DØ collaborations: R. Culbertson, Fermilab-Conf-97-277-E, Proc. SUSY97 (to be published).

21. M. Guchait and D.P. Roy, Phys. Rev. D52, 133 (1995).

22. H. Baer, C. Chen, F. Paige and X. Tata, Phys. Rev. D52, 2746 (1995).

Figure Captions

Fig. 1. The triviality bounds on the Higg boson mass corresponding to differnt cut-off scales, i.e. TeV, GUT and Planck scales.

Fig. 2. The upper and lower bounds on the mass of the SM Higgs boson as functions of the cutoff scale [4].

Fig. 3. Total decay width and the main branching ratios of the SM Higgs boson [8].

Fig. 4. Production cross-sections of the SM Higgs boson at LHC [8].

Fig. 5. The expected significance level of the SM Higgs signal at LHC over the intermediate mass region [9].

Fig. 6. Masses of the MSSM Higgs boson h^0, H^0 and $H^{\pm}$ as functions of the pseudoscalar mass for $\tan\beta = 1.5$ and 30. The predictions without and with maximal stop mixing are shown separately.

Fig. 7. Regions of the parameter space $(M_A - \tan\beta)$ covered by the 5σ discovery contours of various MSSM Higgs signals from the CMS experiment [13].

Fig. 8. Regions of the parameter space $(M_A - \tan\beta)$ covered by the 5σ discovery contours of various MSSM Higgs signals from the combined ATLAS + CMS experiments after 3 years of high luminosity run of LHC [17].

Fig. 9. The expected size of the LSD signals for 300 and 800 GeV gluino production at LHC are shown against the accompanying missing-p_T. The real and fake LSD backgrounds from $\bar{t}t$ production are shown by long dashed and dotted lines respectively [21].

Fig. 10. The expected gluino signals at LHC from jets + missing-E_T channel are shown for $M_{\tilde{g}} \simeq M_{\tilde{q}}$ (squares) and $M_{\tilde{g}} \ll M_{\tilde{q}}$ (triangles). The 95% CL background shown also corresponds to $5\sqrt{B}$ for the LHC luminosity of $10 fb^{-1}$ [22].

Fig. 11. The SUSY discovery limits of various leptonic channels at LHC, where $2\ell\ OS$ and $2\ell\ SS$ denote opposite sign and same sign dileptons [13].

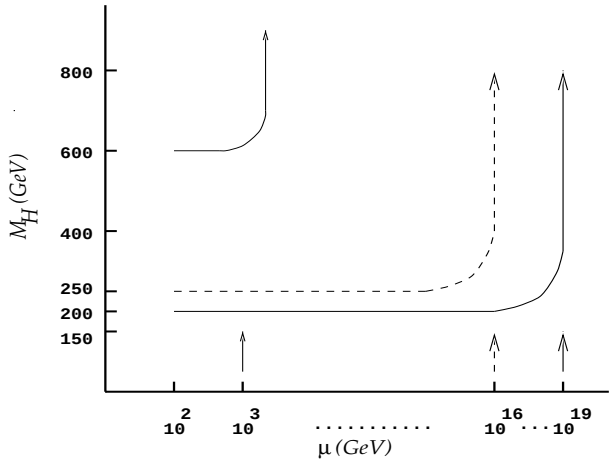

Figure 1: The triviality bounds on the Higg boson mass corresponding to differnt cut-off scales, i.e. TeV, GUT and Planck scales.

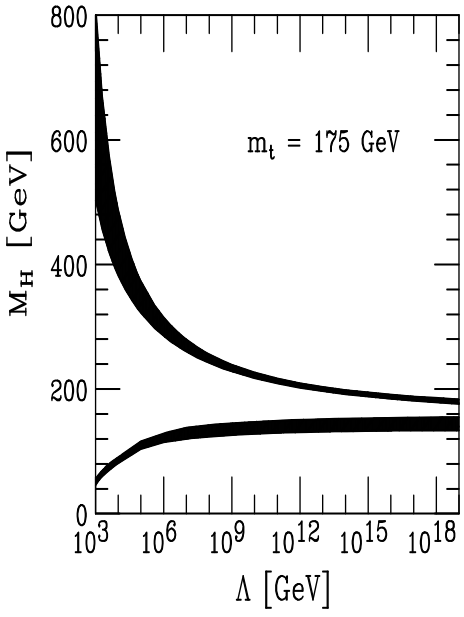

Figure 2: The upper and lower bounds on the mass of the SM Higgs boson as functions of the cutoff scale [4].

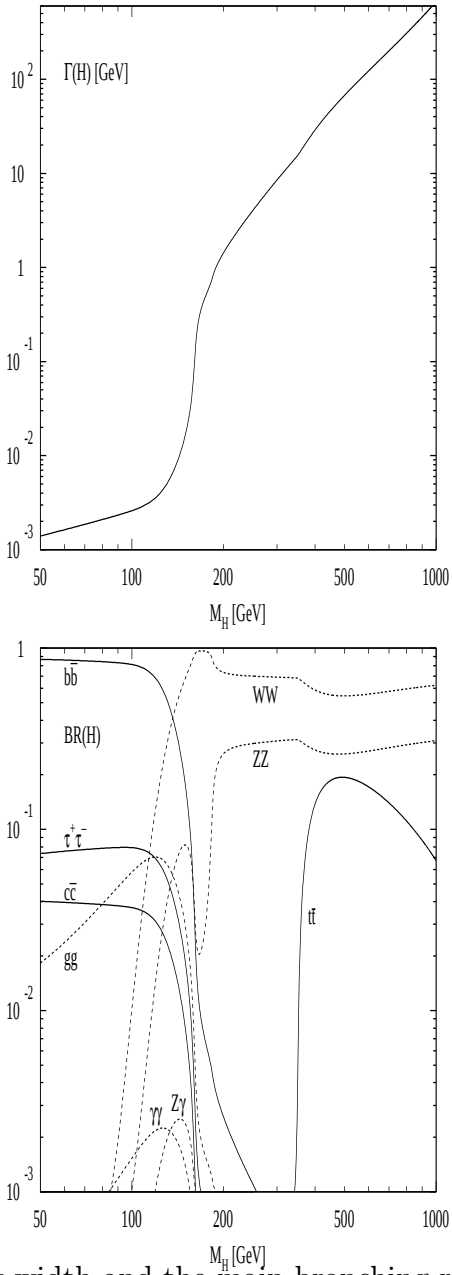

Figure 3: Total decay width and the main branching ratios of the SM Higgs boson [8].

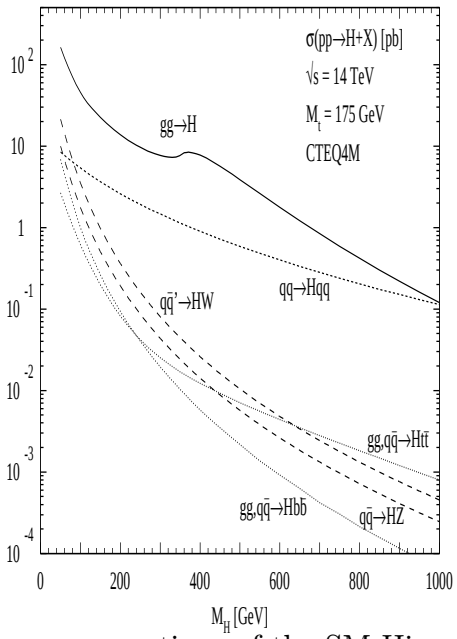

Figure 4: Production cross-sections of the SM Higgs boson at LHC [8].

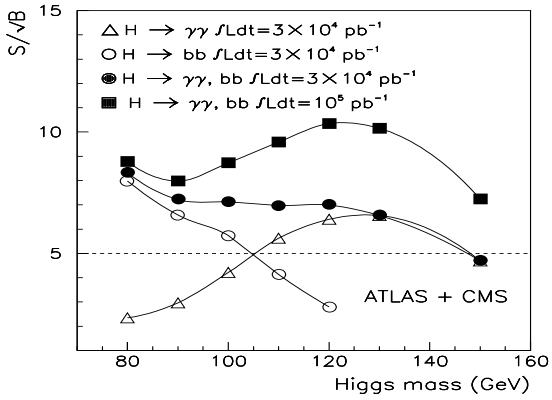

Figure 5: The expected significance level of the SM Higgs signal at LHC over the intermediate mass region [9].

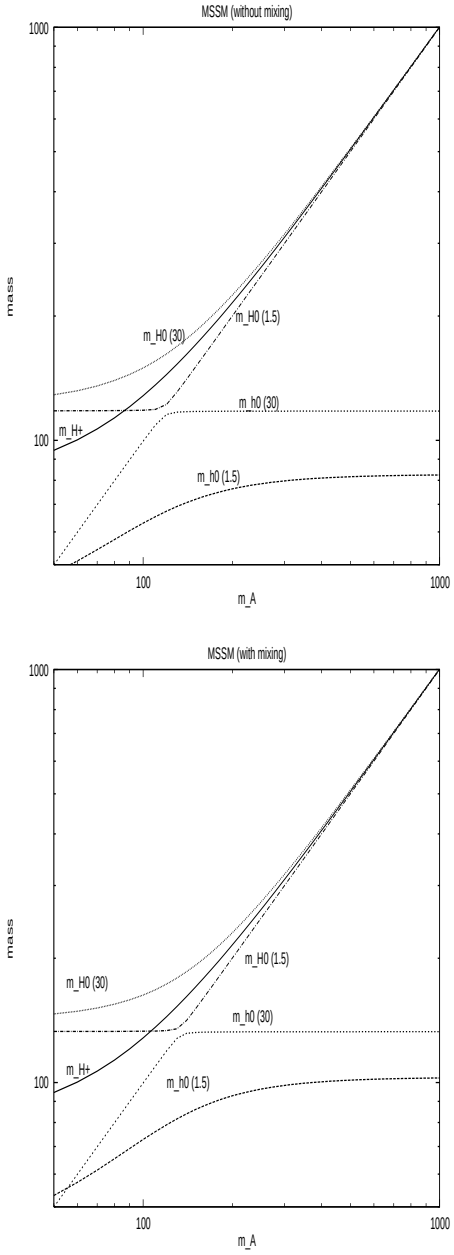

Figure 6: Masses of the MSSM Higgs boson h^0,H^0 and $H^\pm$ as functions of the pseudoscalar mass for $\tan\beta = 1.5$ and 30. The predictions without and with maximal stop mixing are shown separately.

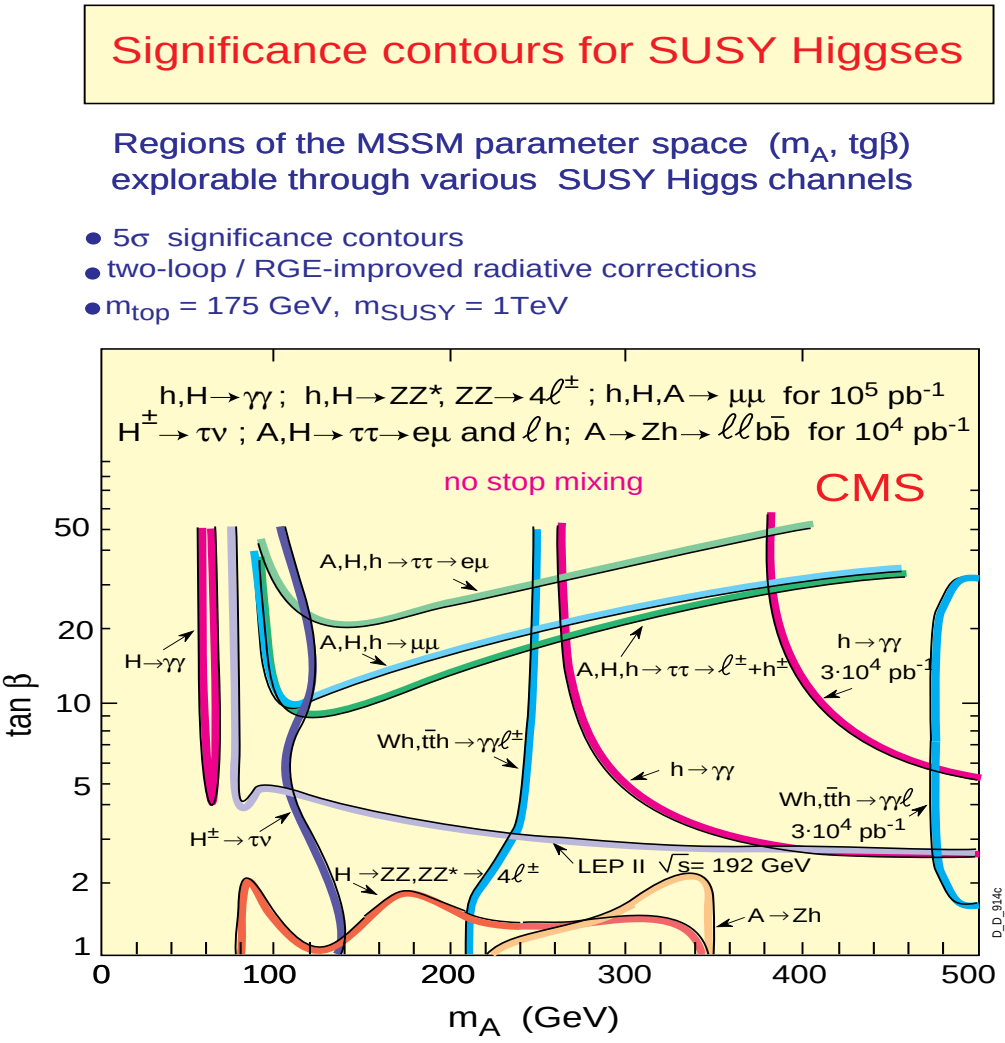

Figure 7: Regions of the parameter space $(M_A - \tan\beta)$ covered by the 5σ discovery contours of various MSSM Higgs signals from the CMS experiment [13].

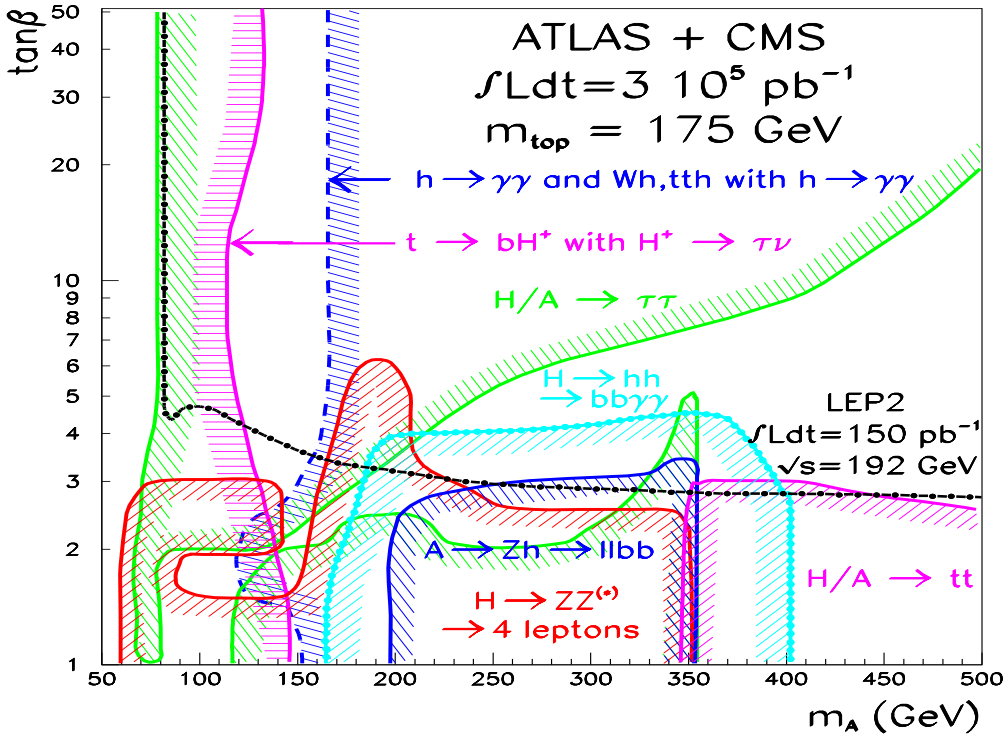

Figure 8: Regions of the parameter space $(M_A - \tan\beta)$ covered by the 5σ discovery contours of various MSSM Higgs signals from the combined ATLAS + CMS experiments after 3 years of high luminosity run of LHC [17].

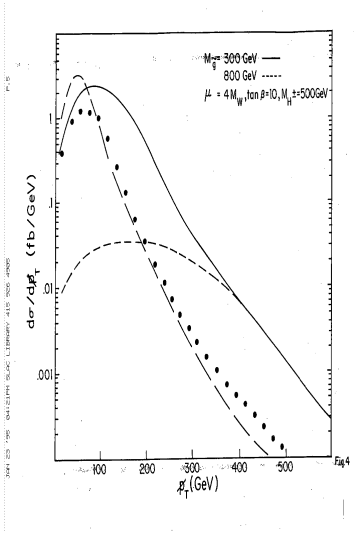

Figure 9: The expected size of the LSD signals for 300 and 800 GeV gluino production at LHC are shown against the accompanying missing-p_T. The real and fake LSD backgrounds from $\bar{t}t$ production are shown by long dashed and dotted lines respectively [21].

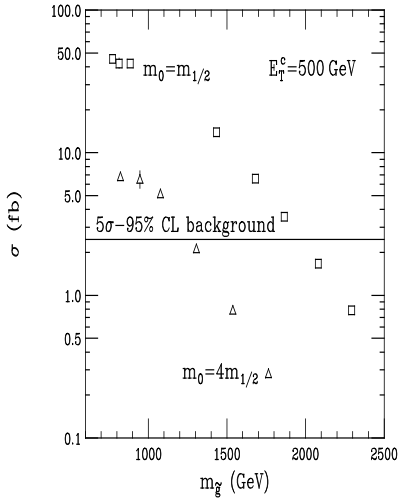

Figure 10: The expected gluino signals at LHC from jets + missing-E_T channel are shown for $M_{\tilde{g}} \simeq M_{\tilde{q}}$ (squares) and $M_{\tilde{g}} \ll M_{\tilde{q}}$ (triangles). The 95% CL background shown also corresponds to $5\sqrt{B}$ for the LHC luminosity of $10 fb^{-1}$ [22].

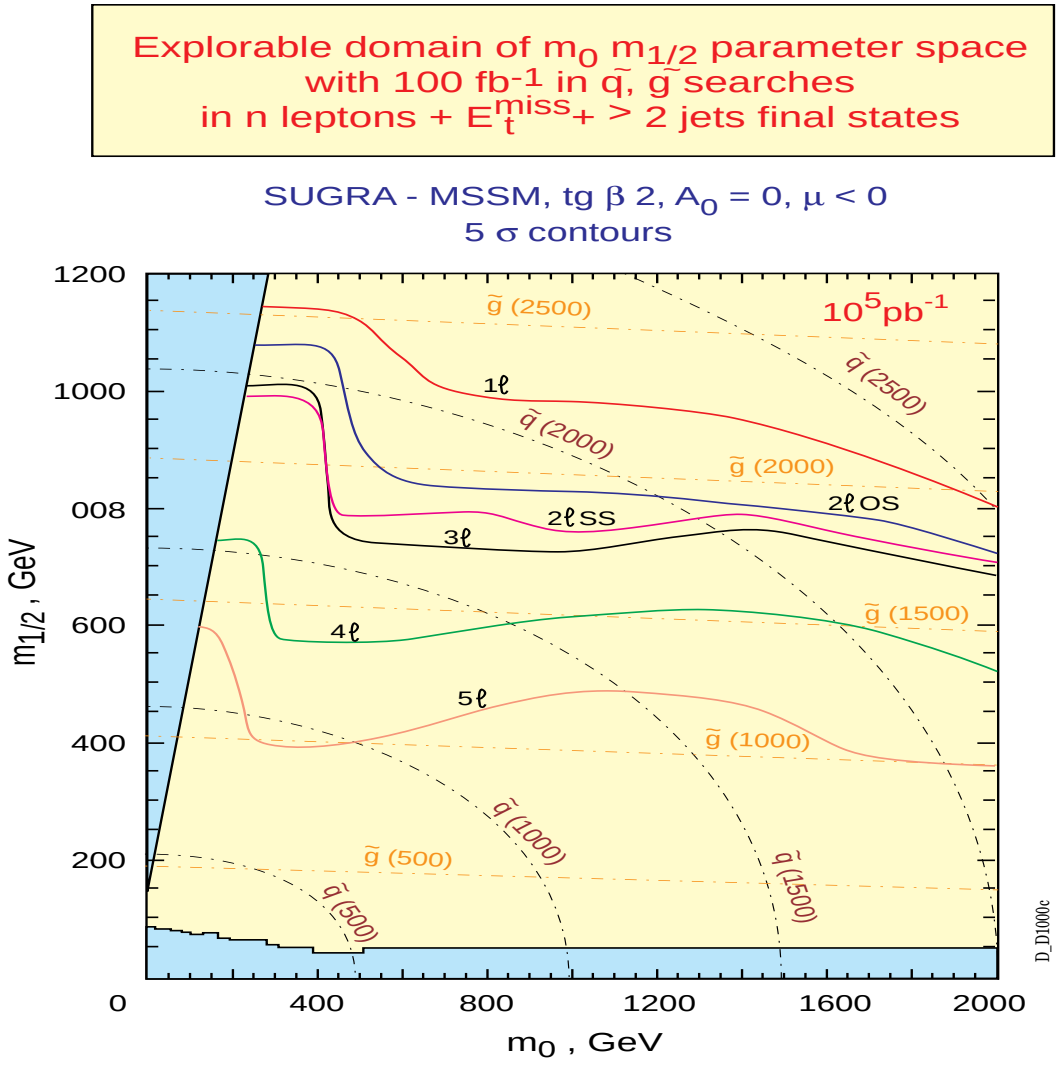

Figure 11: The SUSY discovery limits of various leptonic channels at LHC, where $2l$ OS and $2l$ SS denote opposite sign and same sign dileptons [13].

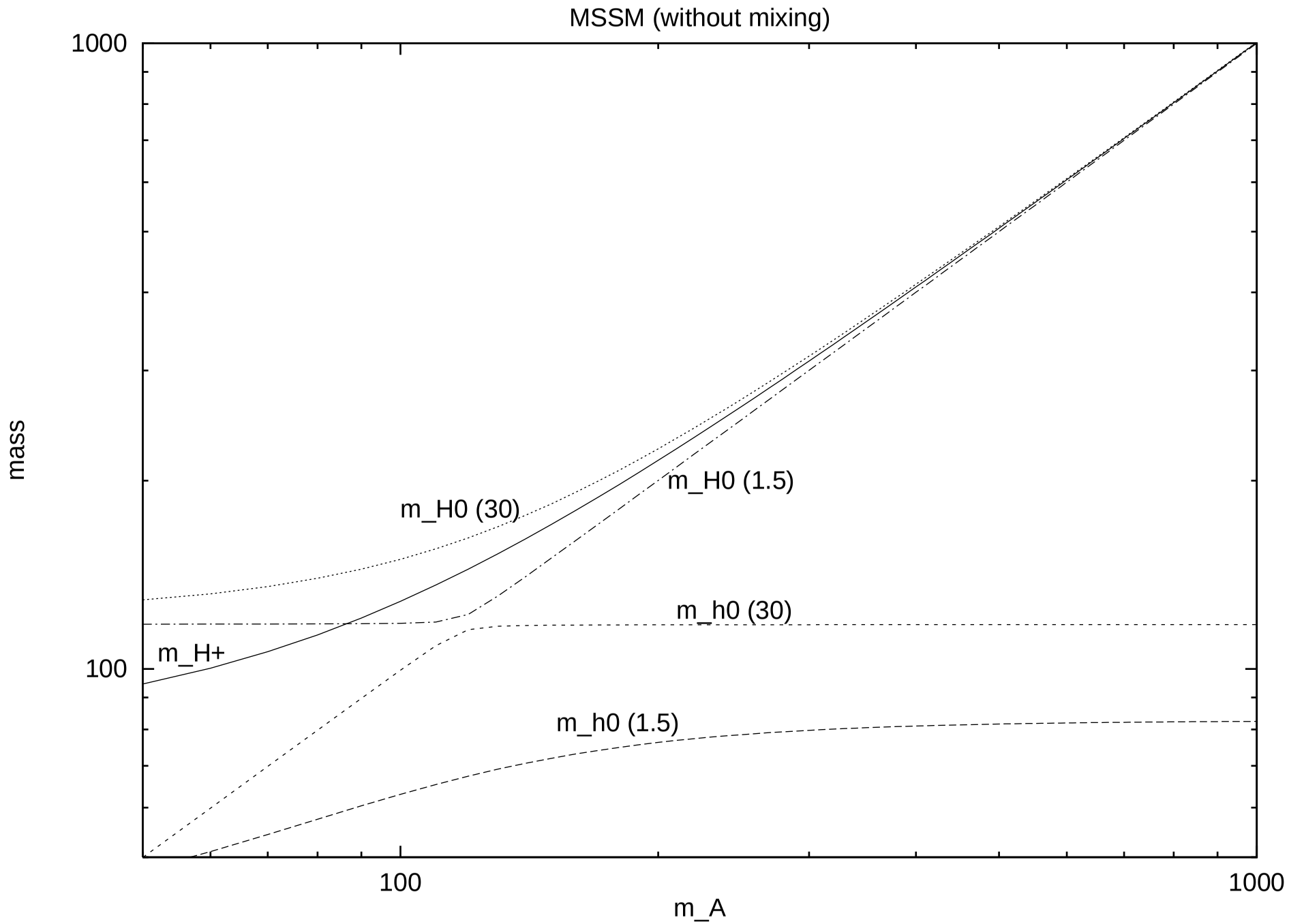
MSSM (without mixing)
1000
100
mass
m_H0 (30)
m_H0 (1.5)
m_h0 (30)
m_H+
m_h0 (1.5)
100
1000
m_A

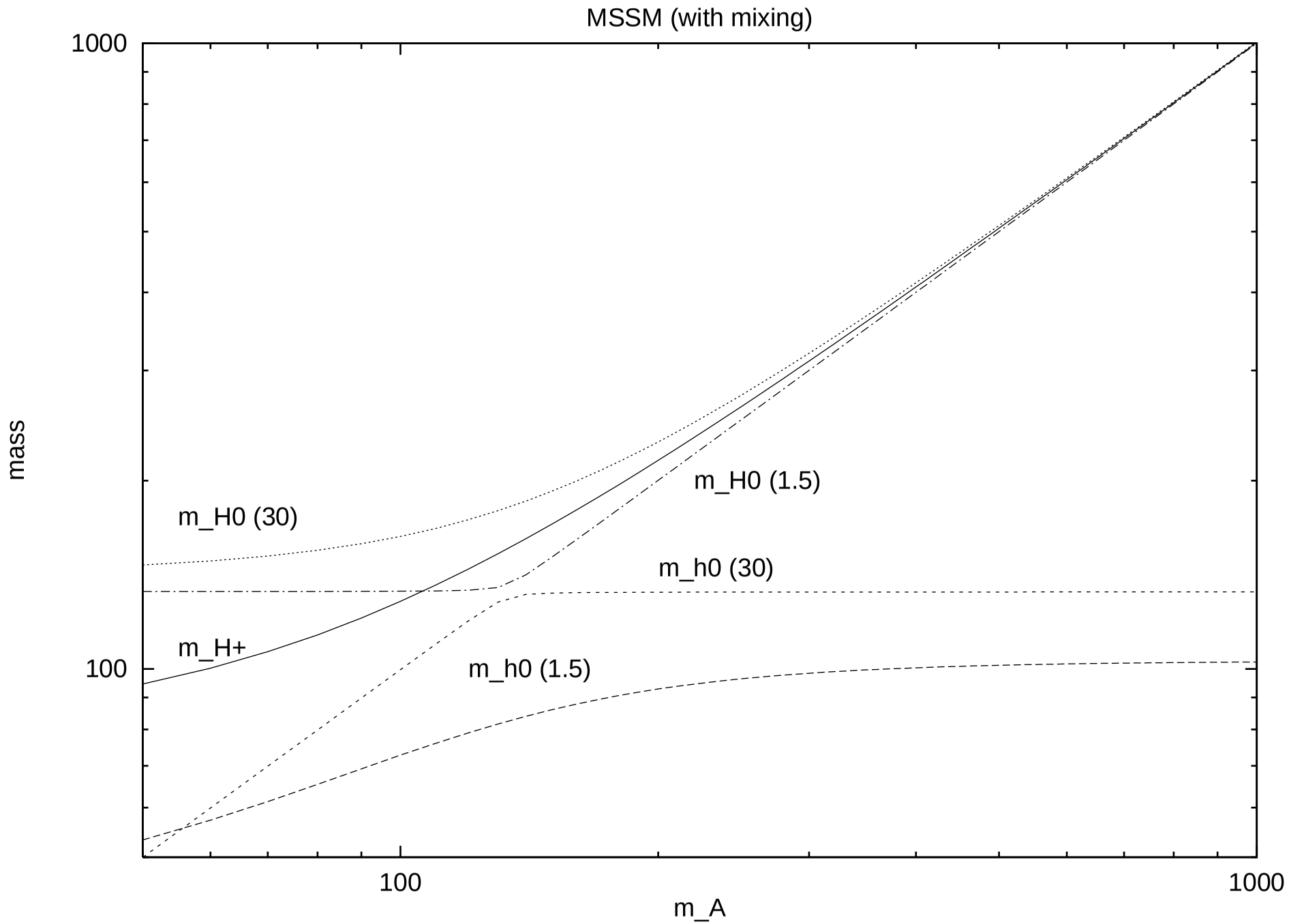
MSSM (with mixing)
1000
100
mass
100
1000
m_A
m_H0 (30)
m_H0 (1.5)
m_h0 (30)
m_H+
m_h0 (1.5)

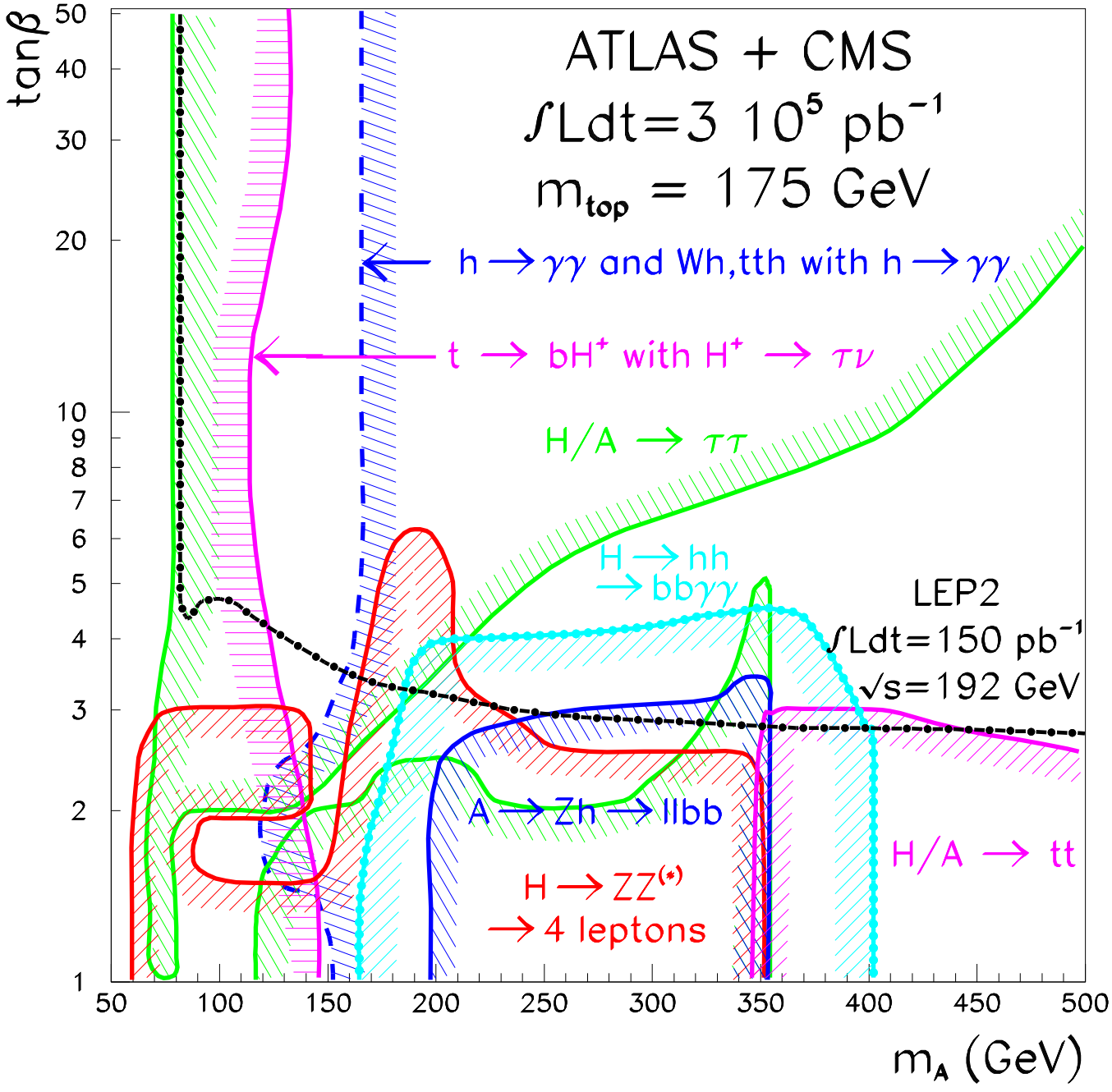
ATLAS + CMS
∫Ldt=3 10⁵ pb⁻¹
m_top = 175 GeV
h → γγ and Wh,tth with h → γγ
t → bH⁺ with H⁺ → τν
H/A → ττ
H → hh
→ bbγγ
LEP2
∫Ldt=150 pb⁻¹
√s=192 GeV
A → Zh → llbb
H/A → tt
H → ZZ(*)
→ 4 leptons
tanβ
m_A (GeV)
50
40
30
20
10
9
8
7
6
5
4
3
2
1
50
100
150
200
250
300
350
400
450
500

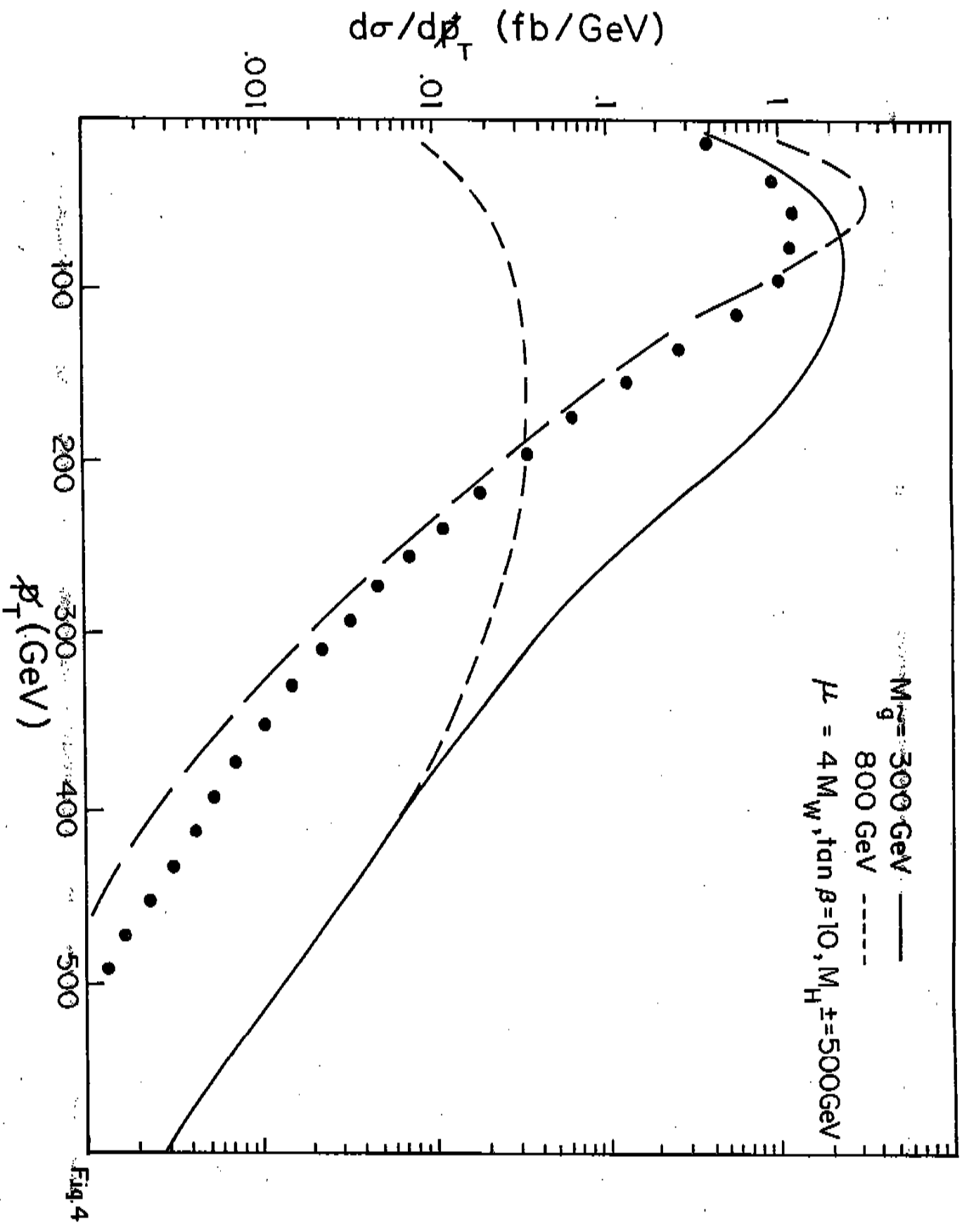
dσ/dp̸_T (fb/GeV)
100
10
1
.1
100
200
300
400
500
p̸_T (GeV)
M_g̃ = 300 GeV
800 GeV
μ = 4M_W, tan β=10, M_H± =500GeV

Fig.4